

ANDRZEJ KOWALSKI*, ELIGIUSZ JĘDRZEJEC*

INFLUENCE OF SUBSIDENCE FLUCTUATION ON THE DETERMINATION OF MINING AREA CURVATURES
WPEŁYW FLUKTUACJI OBNIŻEŃ NA OKREŚLANIE KRZYWIZN TERENU GÓRNICZEGO

The article concerns the random dispersion of deformation indicators, especially the influence of subsidence fluctuation on the distribution of inclinations and curvatures. Surface curvatures have significant influence on building objects. The article includes the probability studies of displacement fluctuation for two arbitrarily close but different points. It was determined, if the probability is dependent on each other or not.

Therefore, the separate deformation indicators can be considered to damage hazard assessment of building objects, if their standard variation of fluctuation is well determined (dependent on the fluctuation of vertical and horizontal displacements). Consequently, it is possible to determine the confidence intervals of fluctuation for all separate deformation indicators. Even in a case of low values of predicted separate curvatures, their values can be significant higher when considering their natural dispersion.

Keywords: mining, land deformation, curvatures, fluctuation, forecast, measurement

Artykuł dotyczy rozproszenia losowego wskaźników deformacji, w szczególności wpływu fluktuacji obniżeń na kształtowanie się fluktuacji nachyleń i krzywizn. W znacznym stopniu dotyczy krzywizn terenu i ich wpływu na obiekty budowlane. Wskaźnika, do którego panują dwa poglądy. Jeden o małej jego przydatności do oceny szkodliwości wpływów eksplotacji górniczej na obiekty budowlane, gdyż w wyniku pomiarów terenowych stwierdza się duży rozrzuł – fluktuacje. Drugi, że wskaźnik ten ma istotne znaczenie, decyduje o zmianie rozkładu pionowych oddziaływań między obiektem a podłożem. Zaznaczyć należy, że wskaźnik ten jest trudno sprawdzalny geodezyjnymi pomiarami. Występowanie fluktuacji – naturalnych rozproszeń – określanych pomiarem wskaźników deformacji tłumaczy się przypadkowym spekaniem górotworu, jego przypowierzchniowej warstwy.

Deformacje odcinkowe wyznaczane z wzorów (1), (2), (3) na podstawie pomiarów przemieszczeń w , u nie są dokładnymi odpowiednikami wskaźników deformacji, które są wynikiem prognozy. Prognowowane wskaźniki deformacji T , K , e , popularnie zwane *wskaźnikami punktowymi*, liczone są w prognozie na podstawie wzorów na pochodne obniżeń i przemieszczeń poziomych w pewnych punktach obliczeniowych. Teoretycznie, oba sposoby byłyby równoważne, gdyby były wyliczane graniczne ich wartości przy długości boku $l \rightarrow 0$.

* CENTRAL MINING INSTITUTE, PLAC GWARKÓW 1, 40-166, KATOWICE, POLAND

W artykule przeanalizowano prawdopodobieństwo fluktuacji przemieszczeń dwóch dowolnie bliskich, lecz różnych punktów, czy jest od siebie zależne, czy też nie.

Najprostsze teoretyczne modele, jakie analizowano są następujące:

- Model igłowy: fluktuacje w dwóch dowolnie bliskich, lecz różnych punktach są od siebie niezależne.
- Model ziarnisty: ośrodek ma strukturę ziarnistą (o różnych rozmiarach ziaren, tak różnorodnie rozmieszczonej, że dowolny punkt (x, y, z) należy zawsze do jakiegoś ziarna lub leży na granicy ziaren sąsiednich).
- Model falisty: można go utworzyć z modelu ziarnistego, co daje obraz podobny do lekko sfalowanego morza. W takim modelu można byłoby rozważyć te fluktuacje, jako ciągłe.

Z analizy tej wynika, że najprostszym i poprawnym w sensie matematycznym jest model falisty, w którym wszystkie pochodne typu (26) są określone z wyjątkiem być może pewnych punktów lub krzywych, gdzie mogą one być nieciągłe. W obszarach, w których są one skończone, podstawową funkcją losową jest fluktuacja obniżeń φ_w . Fluktuacje nachyleń i krzywizn są pochodnymi fluktuacji obniżeń i są jednoznacznie określone przez φ_w . Podobnie jest z poziomymi przemieszczeniami i odkształceniami, gdzie podstawowymi funkcjami losowymi są składowe poziomego przemieszczenia, a fluktuacje odkształceń są wyznaczone przez ich pochodne.

W rozdziale 4, przyjmując różne długości l oraz łączne odchylenie standardowe obniżenia punktu (31 mm) wynikające z błędu pomiaru (1 mm) oraz wynikające z naturalnego rozproszenia (30 mm), obliczono wartości odchyleń standardowych σ_T , σ_K rozproszenia wpływów dla nachyleń i krzywizn. Obliczono je dla wartości ekstremałnych nachyleń $\pm T_{\max}$ oraz krzywizn $\pm K_{\max}$, będących skutkiem przykładowej eksplatacji w postaci półpłaszczyzny, na różnych głębokościach, od 0 do 1000 m, oraz wartości $w_{\max} = 1$ m i parametru r rozproszenia wpływów $r = 300$ m. Obliczenia wartości odchyleń standardowych wykonano przyjmując poziom ufności $\alpha = 0,05$. Wykresy zależności kształtuowania się maksymalnego nachylenia, krzywizny i promienia krzywizny przedstawiono odpowiednio na rysunkach 1-3. Następnie przy założeniu, że wartość odchylenia standardowego σ_w jest niezależna od położenia obiektu względem eksplatacji, obliczono rozkłady obniżeń, nachyleń i krzywizn w całym obszarze wpływów eksplatacji od $1,5r$ do $-1,5r$, co przedstawiono odpowiednio na rysunkach 4-6. Z rysunków tych wynika, jak w znacznym zakresie mogą fluktuować (z prawdopodobieństwem 95%) nachylenia, a zwłaszcza krzywizny w stosunku do wartości średnich, które prognozujemy.

W konkluzji stwierdzono, że o rozproszeniu naturalnym wskaźników nie wiadomo wszystkiego i możliwe są różne podejścia do opisu tego rozproszenia. Z powodu braku wiarygodnego modelu nie jest możliwe określenie odchyleń standardowych w przypadku tzw. punktowych deformacji prognozowanych. Dlatego do oceny zagrożenia obiektów budowlanych można rozpatrywać odcinkowe wskaźniki deformacji, dla których istnieją dobrze określone oszacowania (5), (6), (7) odchyлеń standardowych ich fluktuacji wynikające z ich uzależnienia od fluktuacji obniżeń i przemieszczeń poziomych. W konsekwencji można określić przedziały ufności dla tych fluktuacji dla wszystkich odcinkowych wskaźników deformacji. Nawet w przypadku, gdy prognozowane odcinkowe krzywizny mają bardzo małe wartości, to w wyniku uwzględnienia rozproszenia naturalnego ich wartości mogą być istotnie duże.

Słowa kluczowe: eksplatacja górnicza, deformacja powierzchni, krzywizny, fluktuacja, prognoza, pomiar

1. Introduction

Issues concerning observed random dispersion of deformation indicators have been researched by a number of authors, in chronological order: Batkiewicz, Popiołek, Milewski, Ostrowski, Kwiatek, Stoch and Kowalski.

Batkiewicz (1971) reviewed various formulas of centre which caused random dispersion of deformation indicators. These assumptions and formulas were later continued by: (Popiołek 1976, 1996; Popiołek et al., 1997a,b; Ostrowski, 2006; Stoch, 2005; Popiołek & Stoch, 2005). They recognized quantities of the dispersion occurring in practice and suggested coefficients of variation as its measure. Works developed by Kowalski focused on research concerning this phenomenon (Kowalski, 2007) and he included it in the forecast (Kowalski, 2014).

Research conducted by Kwiatek considered methods that would include these phenomena in methodology of building protection against mining influences. Summary of this research is included in monographs (Kwiatek et al., 1997) and (Kwiatek, 2007), and publications (Kwiatek, 2006, 2008). They mainly relate to land curvatures and the influence they have on buildings. On one hand, it is thought that such indicator is of a small value while estimating a harmfulness level of mining operations on buildings, because field measurements show a great level of dispersion – fluctuations – of obtained curvatures (Popiolek et al., 1995). On the other hand, such indicator has a significant value and decides on a change in distribution of vertical impacts between a building and foundation. In the case of buildings that are not resistant enough, the influence of curvatures causes typical damages (Kwiatek, 2007). It is difficult to accurately check the indicator, however, it is indispensable for building construction on mining areas (Kwiatek, 2006; Florkowska, 2011, 2012).

In addition to curvatures, this paper discusses all other deformation indicators. Therefore, other deformation indicators have been included in this paper with an emphasize on the issues relating to curvatures.

2. Measured deformation indicators

In practice, only differences between measuring point's height and distance L_i of subsequent points of measuring line $i - 1, i^1$ are directly measured. Sometimes the length, angles and differences in height are measured for a closed network of measuring points that allow leveling their coordinates. In both cases such measurements enable to determine the level of point subsidence w_i inclinations T_i of measure bases and curvatures K_i (as relative changes of inclinations of two adjacent bases) at specific times. Additionally, length measurements of measured bases allow determining relative changes of such distances, which is a horizontal deformation. When the points coordinates are determined, it is possible to additionally calculate components of horizontal displacement.

The paper analyses indicators that are dependent on subsidence (inclination and curvatures) and are calculated as:

$$T_i = \frac{w_i - w_{i-1}}{L_i} \quad (1)$$

$$K_i = \frac{T_i - T_{i-1}}{\frac{L_i + L_{i-1}}{2}} \quad (2)$$

and horizontal deformation most often calculated as relative continuation of a section at a time of measurement L'_i in relation to its initial length L_i (1.3).

$$\varepsilon_i = \frac{L'_i - L_i}{L_i} \quad (3)$$

or less often, when components of horizontal point displacements u_x, u_y are counted as:

¹ such sections are also referred to as measured bases.

$$\varepsilon_{x_i} = \frac{u_{x_i} - u_{x_{i-1}}}{\Delta x_i} \quad \text{if } \Delta x_i \neq 0 \quad (4)$$

$$\varepsilon_{y_i} = \frac{u_{y_i} - u_{y_{i-1}}}{\Delta y_i} \quad \text{if } \Delta y_i \neq 0$$

Determined subsidence and horizontal displacement of measured line points, apart from (minor) errors resulting from a measure technique, include also so-called *natural dispersion*. Accidental cracked rock mass is considered to be the cause of such dispersion.

The following issues have not been researched yet:

- whether the dispersion occurs independently of frequency of measurements or whether there are specific areas where the dispersion takes places in a regular (smooth) manner²;
- what is the probability distributions of natural dispersion of separate deformation indicators,
- whether the parameters of such distributions are the same in different locations of subsidence trough.

Values of inclinations, curvatures and horizontal deformations are calculated by the formulas (1)...(4) and are characterised also by natural dispersion of vertical and horizontal displacement.

The work (Kowalski 2007) presents detailed introduction of relations between fluctuation standard deviation σ_T , σ_K , σ_ε of discussed deformation indicators depending on standard deviations σ_w of vertical and horizontal displacements (including measured errors).

In case when $L_i = l$ (for curvatures $L_i = L_{i-1} = l$) standard deviation amounts to:

$$\sigma_T = \frac{\sqrt{2}}{l} \sigma_w \quad (5)$$

$$\sigma_K = \frac{\sqrt{6}}{l^2} \sigma_w \quad (6)$$

$$\sigma_\varepsilon = \frac{\sqrt{2}}{l} \sigma_u \quad (7)$$

(5) and (6) show that:

$$\sigma_K = \frac{\sqrt{3}}{l} \sigma_T \quad (8)$$

and not $\frac{\sqrt{2}}{l} \sigma_T$ as it could be calculated for the formula (2), because in this case random variables T_i , T_{i-1} are not independent (both are dependent on subsidence w_{i-1}).

² smooth dispersion would indicate an existence of certain center block that are moved as a whole, and potentially deformed in a regular manner

If the coefficient of variation is defined acc. to Popiołek (1976) as:

$$\begin{aligned}
 M_w &= \frac{\sigma_w}{w_{\max}} \\
 M_u &= \frac{\sigma_u}{u_{\max}} \\
 M_T &= \frac{\sigma_T}{T_{\max}} \\
 M_K &= \frac{\sigma_K}{K_{\max}} \\
 M_\varepsilon &= \frac{\sigma_\varepsilon}{\varepsilon_{\max}}
 \end{aligned} \tag{9}$$

is calculated by (9):

$$\begin{aligned}
 \frac{M_T}{M_w} &= \frac{\sigma_T}{\sigma_w} \frac{w_{\max}}{T_{\max}} \\
 \frac{M_K}{M_w} &= \frac{\sigma_K}{\sigma_w} \frac{w_{\max}}{K_{\max}} \\
 \frac{M_\varepsilon}{M_u} &= \frac{\sigma_\varepsilon}{\sigma_u} \frac{u_{\max}}{\varepsilon_{\max}}
 \end{aligned} \tag{10}$$

Budryk-Knothe theory shows that:

$$\begin{aligned}
 \frac{w_{\max}}{T_{\max}} &= r \\
 \frac{w_{\max}}{K_{\max}} &= r^2 \sqrt{\frac{e}{2\pi}} \\
 \frac{u_{\max}}{\varepsilon_{\max}} &= r \sqrt{\frac{e}{2\pi}}
 \end{aligned} \tag{11}$$

Therefore, after considering relations (5)...(7) and (11) in (10), the result amounts to:

$$\begin{aligned}
 \frac{M_T}{M_w} &= \frac{\sqrt{2}}{\lambda} \\
 \frac{M_K}{M_w} &= \frac{1}{\lambda^2} \sqrt{\frac{3e}{\pi}} \cong \frac{1.61}{\lambda^2} \\
 \frac{M_\varepsilon}{M_u} &= \frac{1}{\lambda} \sqrt{\frac{e}{\pi}} \cong \frac{0.93}{\lambda^2}
 \end{aligned} \tag{12}$$

where are determined:

$$\lambda = \frac{l}{r} \quad (13)$$

An average outcome of research by Popiółek (1976), Kowalski (2007) and Stoch (2005) shows that:

$$\frac{M_K}{M_w} = \frac{0.46}{0.03} = 15.33$$

$$\frac{M_T}{M_w} = \frac{0.11}{0.03} = 3.67$$

$$\frac{M_\varepsilon}{M_u} = \frac{0.25}{0.09} = 2.78$$

and they are not dependent on λ .

It should be noted that section deformations calculated by the formulas (1)...(3) on the basis of displacement measurements w, u are not accurate equivalents of deformation indicators resulting from forecast. Deformation indicators T, K, ε so called *point indicators*, are calculated on the basis of formulas for derivatives of vertical and horizontal displacements in certain calculation points. Theoretically, both methods would be equivalent if the formulas (1)...(3) contained subsidence derived from a theoretical M model, and instead of the right sides of formulas, their limit values were calculated as the side length approaches to zero $l \rightarrow 0$. Then, obtained values would be equal to T, K, ε values calculated from M model.

When it is assumed, however, that the forecast corresponds exactly to smooth (without any fluctuations) measurement, the estimated point deformation indicators are not much different than section indicators in the case of correspondingly small distances $l \leq 25 \text{ m}^3$.

3. Forecast deformation indicators and their natural dispersion

Estimated deformation indicators of continuous rock mass are calculated by formulas such as Budryk-Knothe theory (Prusek & Jędrzejec, 2008) treated as constant component of actual rock mass deformation indicators⁴, to which statistical fluctuations should be added due to the lack of certainty concerning the theory parameters and statistical fluctuations resulting from *natural dispersion* of corresponding deformation indicators. When a systematic error of theoretical model is neglected, the following aspects can be stated for indicators dependent on the field of vertical and horizontal displacement.

$$w'^z(x, y, z, t) = w(x, y, z, t, P^{pr}) + \Theta_w(x, y, z, t) + \varphi_w(x, y, z, t) \quad (14)$$

$$\begin{aligned} u'_x(x, y, z, t) &= u_x(x, y, z, t, P^{pr}) + \Theta_{u_x}(x, y, z, t) + \varphi_{u_x}(x, y, z, t) \\ u'_y(x, y, z, t) &= u_y(x, y, z, t, P^{pr}) + \Theta_{u_y}(x, y, z, t) + \varphi_{u_y}(x, y, z, t) \end{aligned} \quad (15)$$

³ the greatest differences of point and section inclinations for half-planes when $r = 500 \text{ m}$, $l = 25 \text{ m}$ are 3,8% T_{\max} , and differences of individual curvatures are 20,6% K_{\max}

⁴ which center is complex, partially cracked, partially constant.

$$\begin{aligned} T_x^{rz}(x, y, z, t) &= T_x(x, y, z, t, P^{pr}) + \Theta_{T_x}(x, y, z, t) + \varphi_{T_x}(x, y, z, t) \\ T_y^{rz}(x, y, z, t) &= T_y(x, y, z, t, P^{pr}) + \Theta_{T_y}(x, y, z, t) + \varphi_{T_y}(x, y, z, t) \end{aligned} \quad (16)$$

$$\begin{aligned} \varepsilon_z^{rz}(x, y, z, t) &= \varepsilon_z(x, y, z, t, P^{pr}) + \Theta_{\varepsilon_z}(x, y, z, t) + \varphi_{\varepsilon_z}(x, y, z, t) \\ \varepsilon_{xx}^{rz}(x, y, z, t) &= \varepsilon_{xx}(x, y, z, t, P^{pr}) + \Theta_{\varepsilon_{xx}}(x, y, z, t) + \varphi_{\varepsilon_{xx}}(x, y, z, t) \\ \varepsilon_{yy}^{rz}(x, y, z, t) &= \varepsilon_{yy}(x, y, z, t, P^{pr}) + \Theta_{\varepsilon_{yy}}(x, y, z, t) + \varphi_{\varepsilon_{yy}}(x, y, z, t) \end{aligned} \quad (17)$$

$$\begin{aligned} K_{xx}^{rz}(x, y, z, t) &= K_{xx}(x, y, z, t, P^{pr}) + \Theta_{K_{xx}}(x, y, z, t) + \varphi_{K_{xx}}(x, y, z, t) \\ K_{xy}^{rz}(x, y, z, t) &= K_{xy}(x, y, z, t, P^{pr}) + \Theta_{K_{xy}}(x, y, z, t) + \varphi_{K_{xy}}(x, y, z, t) \\ K_{yy}^{rz}(x, y, z, t) &= K_{yy}(x, y, z, t, P^{pr}) + \Theta_{K_{yy}}(x, y, z, t) + \varphi_{K_{yy}}(x, y, z, t) \end{aligned} \quad (18)$$

where:

- $w^{rz}, T^{rz}, K^{rz}, \varepsilon^{rz}$ — actual rock mass deformation indicators,
- $P = (P_1, P_2, \dots, P_m)$ — m set of theory parameters,
- P^{pr} — a set of these parameters with values used for forecast,
- w, T, K — constant rock mass deformation indicator calculated for values of P_{pr}
- theory parameters adopted for the forecast,
- $\Theta_{...}(x, y, z, t)$ — random functions showing the impact of *uncertain theory parameters*
- on individual deformation indicators,
- $\varphi_{...}(x, y, z, t)$ — random functions showing the impact of *natural dispersion* of individual deformation indicators.

Theory parameters adopted for the forecast are never entirely certain, unless the values are verified by deformation indicators measurement taken after mining operations. Approximation of this parameter conducted acc. to the theory results in parameters values P^{dok} , referred to as accurate. Their values are unknown at the time of the forecast. Shall:

$$\Delta P_k = P_k^{dok} - P_k^{pr}, \quad k = 1, 2, \dots, m \quad (19)$$

$$\Delta P = (\Delta P_1, \Delta P_2, \dots, \Delta P_m) \quad (20)$$

It can be said that $\Theta_{...}(x, y, z, t)$ functions:

- would be equal to zero if the theory parameters were certain,
- are continuous and their values are $\Omega_{\Theta_{...}} = (-\infty, +\infty)$ real numbers,
- it can be assumed that the distribution of their probability are constant and their density $\rho_{\Theta_{...}}$ is even-numbered — they are symmetrical $\rho_{\Theta_{...}}(-\Theta_{...}) = \rho_{\Theta_{...}}(\Theta_{...})$ ⁵,
- it can be assumed that distributions of difference probability ΔP_k are normal with zero average values,
- their values equal zero.

⁵ what results from assumption that the probability of deviation is independent from its sign

In fact, for instance, for subsidence occurs:

$$\Theta_w(x, y, z, t) = w(x, y, z, t P^{dok}) - w(x, y, z, t P^{pr}) \quad (21)$$

Considering (2.5), it can be described as:

$$\Theta_w(x, y, z, t) = w(x, y, z, t P^{pr} + \Delta P) - w(x, y, z, t P^{pr}) \quad (22)$$

For minor difference, ΔP_k the formula (2.8) can be approximated by linear formula:

$$\Theta_w(x, y, z, t) = \sum_{k=1}^m \left[\frac{\partial w(x, y, z, t, P)}{\partial P_k} \Big|_{P^{pr}} \Delta P_k \right] \quad (23)$$

Assuming that errors ΔP_k are not dependent, the variation $\sigma_{\Theta_w}^2$ can be calculated as:

$$\sigma_{\Theta_w}^2(x, y, z, t) = \sum_{k=1}^m \left[\left(\frac{\partial w(x, y, z, t, P)}{\partial P_k} \Big|_{P^{pr}} \right)^2 \sigma_{P_k}^2 \right] \quad (24)$$

Generally, the differences ΔP_k can not be recognized as small enough and as a result, the issue remains non-linear:

$$\begin{aligned} \sigma_{\Theta_w}^2(x, y, z, t) &= E(\Theta_w^2) = \\ &= \int_{\Omega_{P_1}} \dots \int_{\Omega_{P_m}} [w(x, y, z, t P^{pr} + \Delta P) - w(x, y, z, t P^{pr})]^2 \rho_P d(\Delta P_1) \dots d(\Delta P_m) \end{aligned} \quad (25)$$

where Ω_{P_k} is the error range ΔP_k , and $\rho_P(\Theta_w)$ is the distribution density of deviation Θ_w probability.

If the errors ΔP_k are independent, then:

$$\rho_P = \prod_{k=1}^m \rho_{P_k}$$

where ρ_{P_k} are densities of error distribution ΔP_k .

Equalities analogical to (21)..(25) occur for the other deformation indicators.

It is noteworthy, that standard deviation is a function of the position $\sigma_{\Theta_{...}} = \sigma_{\Theta_{...}}(x, y, z, t)$.

For established realisation of random variables ΔP functions $\Theta_{...}$ are certain continuous surfaces in the whole range of exploitation influences, whereas it has not been decided whether their fluctuation realisation $\varphi_{...}$ is of a continuous character. Due to the fact that the measurements are taken at locations where the points are located in certain distances, it is unknown how fluctuation occurs in two randomly located points. In particular, it has not been determined if the probability of fluctuation occurring at a point is depended on another randomly located point.

The simplest theoretical models that seem to be up-to-date can be characterised by:

- Needle Model: fluctuations in two randomly located, but different, points. It means that they have an image of independent ‘needles’ in each measuring point in the whole area of exploitation influences (an image similar to ‘signal noise’). If the measuring points

were located in every point of the location impacted by mining operations (in a form of *dense-in-itself mosaic*), the image of the functions would represent *dense-in-itself 'bush of needles'* with random amplitudes.

- **Granular Model:** the centre has granular structure (with varied granularity and randomly located so that any point (x, y, z) always belongs to a grain or is located at the border of neighbouring grains, because, if a local empty space was created as a result of such centre deformation, it may be recognized as a separate grain), and fluctuations have forms locally continuous (in the area of grains) surfaces – prisms with random heights, with bases as curvilinear outlines of grains and tips in a form of certain continuous surfaces.
- **Corrugated Model:** it may be created from the Granular Model by applying certain continuous surface on continuous surface of fluctuation $\varphi_{...}$ (resulting in lightly wavy sea). The functions in such model could be considered as continuous.

Discussion often concerning the problem includes an idea that fluctuations $\varphi_{...}$ are independent of a location in the case of fluctuations probability that would be identical in sides of a subsidence trough as well as its centre. It has not, however, been proved by any research.

Other theories would also seem justified, such as that the probability is proportional to the size or maximum size of an adequate deformation indicator. Generally, it is safe to assume that the probability is dependent on the location and such dependency can be determined by appropriate research.

The state (set) of fluctuation $\varphi_{...}$ at the t moment must have a form of function dependent on the location in the whole area of exploitation influences, otherwise, they would all have the same value which is contrary to observations.

It can be said that $\varphi_{...}(x, y, z, t)$ functions:

- the values at t moment belong to a continuous and cohesive set of real numbers $\Omega_{\varphi_{...}}$ ⁶,
- it can be assumed that the distribution of their probability is constant and their density $\rho_{\varphi_{...}}$ is even-numbered, as a result $\rho_{\varphi_{...}}(-\varphi_{...}) = \rho_{\varphi_{...}}(\varphi_{...})$ ⁷,
- their average values equal zero.

In the case of the Granular Model, the set of function characteristics $\varphi_{...}(x, y, z, t)$ can be extended by a feature – during the realisation t in the area of every grain, they are continuous functions of the location and time, and on the grain borders they may be non-continuous. Such feature results from the fact that components of inclination are derivatives of subsidence, components of curvatures are inclination derivatives and the granular centre can be calculated by adequately small λ .⁸

$$\varphi_{T_x}(x, y, z, t) = \lim_{\lambda \rightarrow 0} \frac{\varphi_w(x + \lambda, y, z, t) - \varphi_w(x, y, z, t)}{\lambda} \quad (26)$$

There are certain possible locations of two points $A = (x, y, z)$ and $B = (x + \lambda, y, z)$, with λ small enough:

1. **A** and **B** point at inside of the same grain:

$\varphi_w(x + \lambda, y, z, t) = \varphi_w(x + \lambda, y, z, t) + \lambda \cdot a(x + \lambda, y, z, t)$ can be added to the linear approximation what gives $\varphi_{T_x} = a$.

⁶ there is a probability that it is a set $(-\infty, +\infty)$

⁷ what results from assumption that the probability of deviation is independent from its sign

⁸ so small that the section $(x, x + \lambda)$ would be located near the grain

2. One of the points shows the inside of a grain, and the other points at its border: the value near the grain or infinitely near to the grain may be assigned to the border function and this still can be connected with the first case.
3. Both points show (always, with random small value of λ) the borders of neighbouring grains (two or more): the value of counter quotient is undetermined, and a value φ_{T_x} in that point – non-continuous.

Similarly, it can be determined that the other derivatives $\varphi_{T_y}, \varphi_{K_{xx}}, \varphi_{K_{xy}}, \varphi_{K_{yy}}$ in the area of every grain, also in the granular centre are continuous functions of the location and time, and on the grain borders they may be non-continuous.

Let in the area of a random grain located at z height, occur at t moment function φ_w , which, if the granularity is small enough, is formed by following equation (accurate to the decimal place):

$$\varphi_w(x, y) = q_0 + q_1x + q_2y + q_3x^2 + q_4xy + q_5y^2 \quad (27)$$

where the coordinate system xy moved in such a way, that coordinates $x = 0, y = 0$ point at the centre of a grain.

Coefficients q_0, q_1, \dots, q_5 are random variables and their realisation at t moment is determined by the continuous function (27). Because a grain is subject to forces moving from neighbouring grains, some or all coefficients q_i may be dependent on each other⁹.

Therefore:

$$\begin{aligned} \varphi_{T_x}(x, y) &= \frac{\partial \varphi_w}{\partial x} = q_1 + 2q_3x + q_4y \\ \varphi_{T_y}(x, y) &= \frac{\partial \varphi_w}{\partial y} = q_2 + q_4x + 2q_5y \end{aligned} \quad (28)$$

$$\begin{aligned} \varphi_{K_{xx}}(x, y) &= \frac{\partial \varphi_{T_x}}{\partial x} = 2q_3 \\ \varphi_{K_{xy}}(x, y) &= \frac{\partial \varphi_{T_x}}{\partial y} = \frac{\partial \varphi_{T_y}}{\partial x} = q_4 \\ \varphi_{K_{yy}}(x, y) &= \frac{\partial \varphi_{T_y}}{\partial y} = 2q_5 \end{aligned} \quad (29)$$

Similar relations can be calculated for displacement components and horizontal deformations.

If a grain is relatively big in relation to the size of measuring base, but small enough to allow measuring point to belong to another grains, local (in the area of the grain) inclinations and curvatures may significantly differ from the ones calculated by formulas (1) and (2). It seems, however, that cracked sections of the centre are moving and turning, but their local curvatures can be omitted. As a result, it is justified to expect that the effects would be registered by properly frequent measurement.

Contrary to this, results of measurements conducted at Kazimierz-Juliusz Mine are presented by Kowalski (2007) indicate that for section $l = 5$ m the curvatures experience is noticeably greater

⁹ for instance, if the grain is stiff enough, so that it cannot bend, it may be assumed that coefficients q_3, q_4, q_5 disappear.

dispersion than in the case longer measurement bases. This would indicate that the grains are smaller than 5 m (for example few centimetres) or actual rock mass (at least in the surface layer) cannot be determined by the Granular Model.

The Needle Model does not include spatial fluctuation derivatives as functions of (26), and fluctuations of inclinations and curvatures should be considered as entirely independent random functions.

The easiest mathematical model is the Corrugated Model, in which all derivatives (26) are determined; in exception of some point or curvatures which may be non-continuous. In the areas where they are non-continuous, the main random function is subsidence fluctuation φ_w . Inclination and curvatures fluctuations are derivatives of subsidence fluctuations and are explicitly determined by φ_w . It is the same in the case of horizontal displacement and deformations, where the basic random functions are components of horizontal displacement, and deformation fluctuations are determined by their derivatives.

4. Probabilistic forecast of deformation indicators

Formulas (14)...(18) can be formulated as:

$$D^{rz}(x, y, z, t) = D(x, y, z, t P^{pr}) + \Theta_D(x, y, z, t) + \varphi_D(x, y, z, t) \quad (30)$$

where D is any deformation indicator from among subsidence, components of horizontal displacement, inclinations and curvatures, as well as vertical deformations and components of horizontal deformations.

A forecasts error of D indicator is marked by:

$$\omega_D = D^{rz}(x, y, z, t) - D(x, y, z, t P^{pr}) \quad (31)$$

and its variation is marked by:

$$E(\omega_D^2) = \sigma_D^2 \quad (32)$$

If ranges of random variables Θ_D , φ_D amount to Ω_{Θ_D} , Ω_{φ_D} and distribution densities are $\rho_{\Theta_D}(\Theta_D)$, $\rho_{\varphi_D}(\varphi_D)$ and because of random variables Θ_D , φ_D are independent, the density of probability that variables take certain values of realization is:

$$\rho_D = \rho_{\Theta_D} \cdot \rho_{\varphi_D} \quad (33)$$

As a result of (30) and (31), due to the fact that random variables Θ_D , φ_D are independent, the following occurs:

$$\sigma_D^2 = \sigma_{\theta_D}^2 + \sigma_{\varphi_D}^2 \quad (34)$$

it results for the following calculation:

$$\begin{aligned}
 E(\omega_D^2) &= \int_{\Omega_{\Theta_D}} \int_{\Omega_{\varphi_D}} (\Theta_D^2 + 2\Theta_D\varphi_D + \varphi_D^2) \rho_{\Theta_D} \cdot \rho_{\varphi_D} d\Theta_D d\varphi_D = \\
 &= \underbrace{\int_{\Omega_{\Theta_D}} \Theta_D^2 \rho_{\Theta_D} d\Theta_D}_{\text{1}} \underbrace{\int_{\Omega_{\varphi_D}} \varphi_D d\varphi_D}_{\bar{\varphi}_D=0} + 2 \underbrace{\int_{\Omega_{\Theta_D}} \Theta_D \rho_{\Theta_D} d\Theta_D}_{\bar{\Theta}_D=0} \underbrace{\int_{\Omega_{\varphi_D}} \varphi_D \rho_{\varphi_D} d\varphi_D}_{\bar{\varphi}_D=0} + \\
 &\quad + \underbrace{\int_{\Omega_{\Theta_D}} \rho_{\Theta_D} d\Theta_D}_{\text{1}} \underbrace{\int_{\Omega_{\varphi_D}} \varphi_D^2 + \rho_{\varphi_D} d\varphi_D}_{\sigma_{\varphi_D}^2} = \sigma_{\Theta_D}^2 + \sigma_{\varphi_D}^2
 \end{aligned} \tag{35}$$

Range of confidence for D deformation indicator at confidence level of α , is determined as follows:

Shall Z occurrence be based on:

$$-q_{1D}(\alpha) \leq D^r - D \leq q_{2D}(\alpha) \tag{36}$$

where:

$$\begin{aligned}
 P(Z) &= \int_{-q_{1D}(\alpha)}^{q_{2D}(\alpha)} \rho_D(\omega_D) d\omega_D = 1 - \alpha \\
 &\text{additionally} \\
 P(\omega_D \leq -q_{1D}(\alpha)) &= \int_{-\infty}^{-q_{1D}(\alpha)} \rho_D(\omega_D) d\omega_D = \frac{\alpha}{2}
 \end{aligned} \tag{37}$$

When the distribution of probability $\rho_D(\omega_D)$ is an even function $s\rho_D(-\omega_D) = \rho_D(\omega_D)$, which occurs when densities $\rho_{\Theta_D}, \rho_{\varphi_D}$ are even functions (which was the subject of assumptions), then as a result:

$$q_{1D}(\alpha) = q_{2D}(\alpha) = q_D(\alpha) \tag{38}$$

and

$$P(|D^r - D| \leq q_D(\alpha)) = \int_{-q_D(\alpha)}^{q_D(\alpha)} \rho_D(\omega_D) d\omega_D = 1 - \alpha \tag{39}$$

Assuming, that distributions $\rho_{\Theta_D}, \rho_{\varphi_D}$ are normal, the distribution ρ_D will be normal with an average equal to zero and variations σ_D^2 determined by the function (34).

As a result, $1 - \alpha$ – fractiles are:

$$q_D(\alpha) = \mu(\alpha)\sigma_D$$

where $\mu(\alpha)$ are independent of deformation indicator; their values presented in Table 1.

TABLE 1

The value of indicator $\mu(\alpha)$, depending on quantiles α and $1 - \alpha$

α	$1 - \alpha$	$\mu(\alpha)$
0.001	0.999	3.290528
0.002700	0.997300	3
0.01	0.99	2.575830
0.02	0.98	2.326348
0.025	0.975	2.241402
0.045500	0.954500	2
0.05	0.95	1.959964
0.1	0.9	1.644854
0.2	0.8	1.281552
0.25	0.75	1.150350
0.317311	0.682689	1
0.5	0.5	0.674490

5. Inclination and curvatures of building foundation – forecast and measurement

An important indicator of deformation for building designers is the curvature of building foundation. In the case of deeper mining excavations, particularly parameters r of influences dispersion, the values of forecast curvatures are small. Consequently, does it mean that measured curvatures are in such cases also small? Authors do not have any measurement of curvatures of such large parameter r that forecast values of maximum curvatures would, for instance, almost equal to values for the zero category of mining areas (in Poland), while the observed ones – would be significantly greater. However, as a result of an analysis of a number of mining operations, Kowalski (2014) stated that generally forecasts of extreme curvatures are systematically too small (50% on average).

Natural, random subsidence fluctuations may be the cause. The following test has been conducted in order to demonstrate possible influence on observed curvatures.

Taking various lengths l of building's foundation (excluding dilatation) and total statistical deviation of point subsidence (31 mm) resulting from a measurement error (1 mm) and natural dispersion (30 mm), calculated the value of standard deviations σ_T , σ_K of influences dispersion for inclination and curvatures. The results are presented in Table 2, which contains emphasized values of typical length $l = 25$ m.

TABLE 2

Calculated values of standard deviations for inclinations and curvatures, depending on the length of measured base

l, m	$\sigma_T, \text{mm/m}$	σ_K, km^{-1}
1	2	3
5	8.77	3.04
10	4.38	0.76
15	2.92	0.34
20	2.19	0.19

1	2	3
25	1.75	0.12
30	1.46	0.08
35	1.25	0.06
40	1.10	0.05

At the confidence level $\alpha = 0.05$ or the typical length l confidence ranges were calculated, assuming that parameters w_{\max} , r are correct and free of any errors:

1. for inclinations $1.959964 \cdot 1.75 \text{ mm/m} = 3.43 \text{ mm/m}$,
2. for curvatures $1.959964 \cdot 0.12 \text{ km}^{-1} = 0.2352 \text{ km}^{-1}$.

Extreme values of inclinations and curvatures will occur for model exploitation in a form of a half-plane located in known areas: $\pm T_{\max}$ and $\pm K_{\max}$. Scheme of relation¹⁰ for such exploitation carried out at different depths characterised by r parameter of influences dispersion and with assumed value $w_{\max} = 1 \text{ m}$.

- for inclinations $T_{\max}(r)$, $T_{\max}(r) + 3.43 \text{ mm/m}$ and $T_{\max}(r) - 3.43 \text{ mm/m}$ (Fig. 1),
- for curvatures $K_{\max}(r)$, $K_{\max}(r) + 0.2352 \text{ km}^{-1}$ and $K_{\max}(r) - 0.2352 \text{ km}^{-1}$ (Fig. 2).

The charts distinct an example value $r = 300 \text{ m}$. Maximum curvatures of such value r are minor (curvature radius = 59.20 km – the zero category of mining area), however, limitations of confidence range become more significant for buildings protection (curvature radius = -4.52 km, 3.92 km – 4th and 5th category of mining terrain).

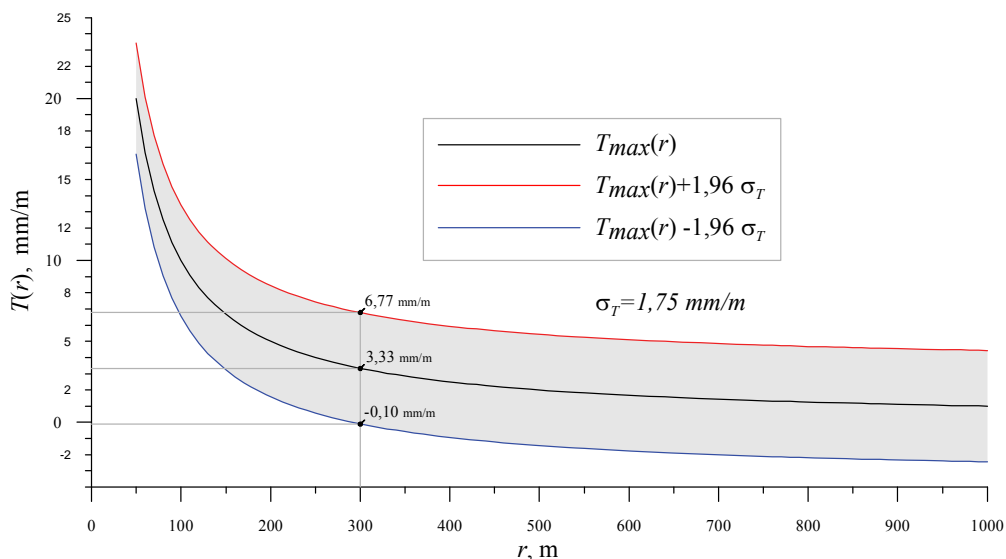


Fig. 1. Chart of the relation of maximum inclination from the parameter r of influences dispersion.

Marked confidence range includes actual value with probability $1 - \alpha = 0.95$
and an example section for $r = 300 \text{ m}$

¹⁰ Positive and negative signs for inclination and curvatures were assumed according to rules using in building industry

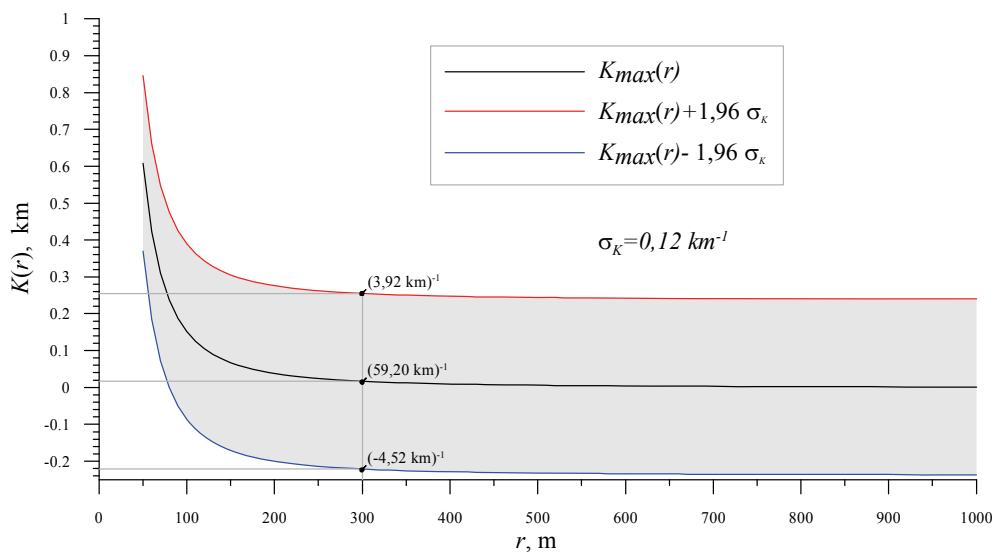


Fig. 2. Chart of the relation of maximum curvatures from the parameter r of influences dispersion.
Marked confidence range includes actual value with probability $1 - \alpha = 0.95$
and an example section for $r = 300$ m

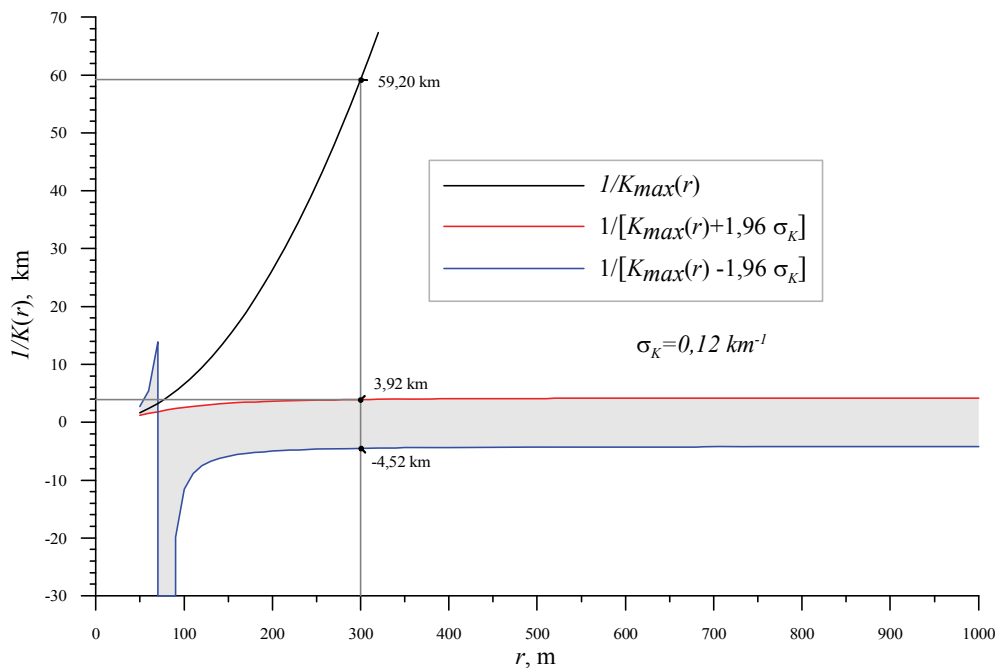


Fig. 3. Chart of the relation of minimum radius for curvatures from the parameter r of influences dispersion.
Marked confidence range includes actual value with probability $1 - \alpha = 0.95$
and an example section for $r = 300$ m

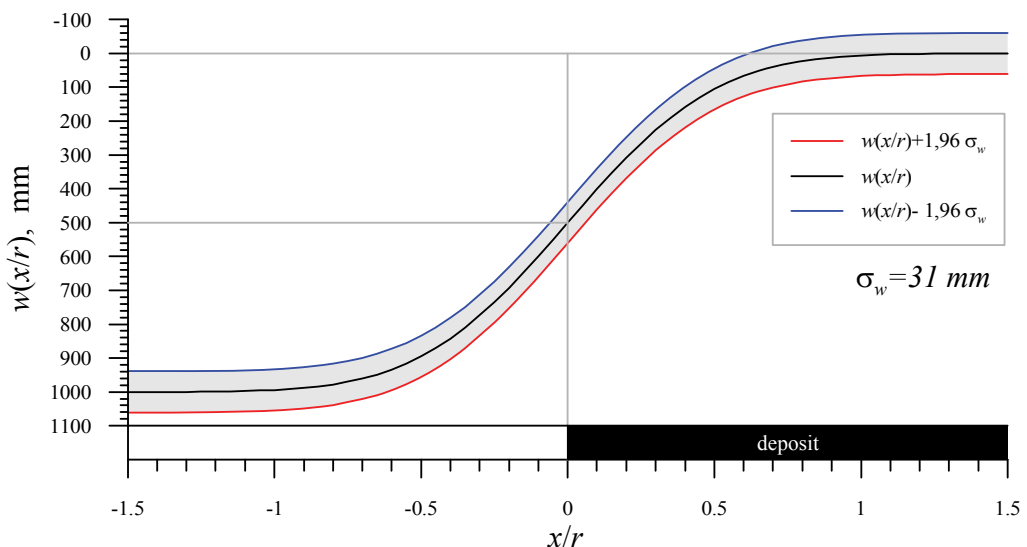


Fig. 4. Chart of subsidence depending on x/r . Marked confidence range includes actual value with probability $1 - \alpha = 0.95$

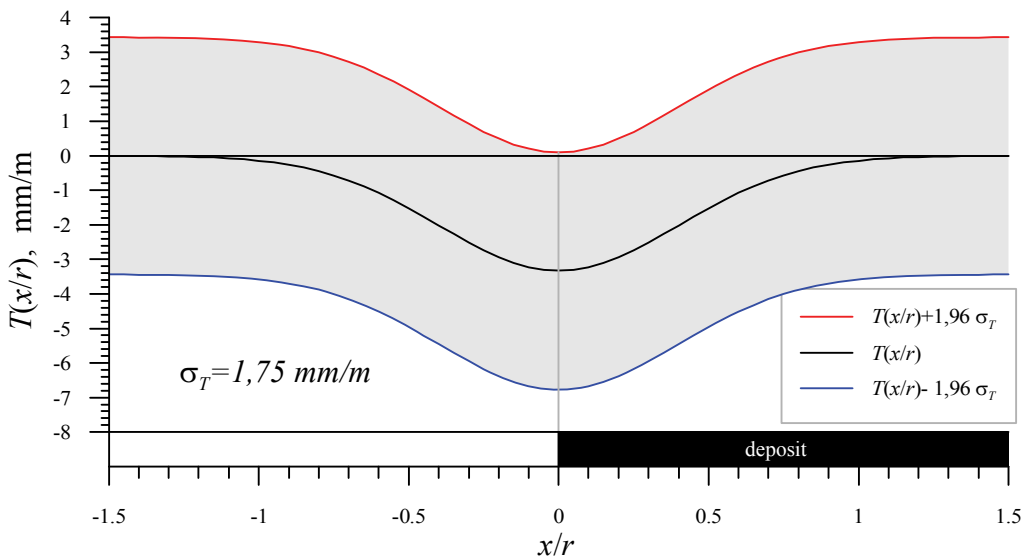


Fig. 5. Chart of inclination depending on x/r . Marked confidence range includes actual value with probability $1 - \alpha = 0.95$

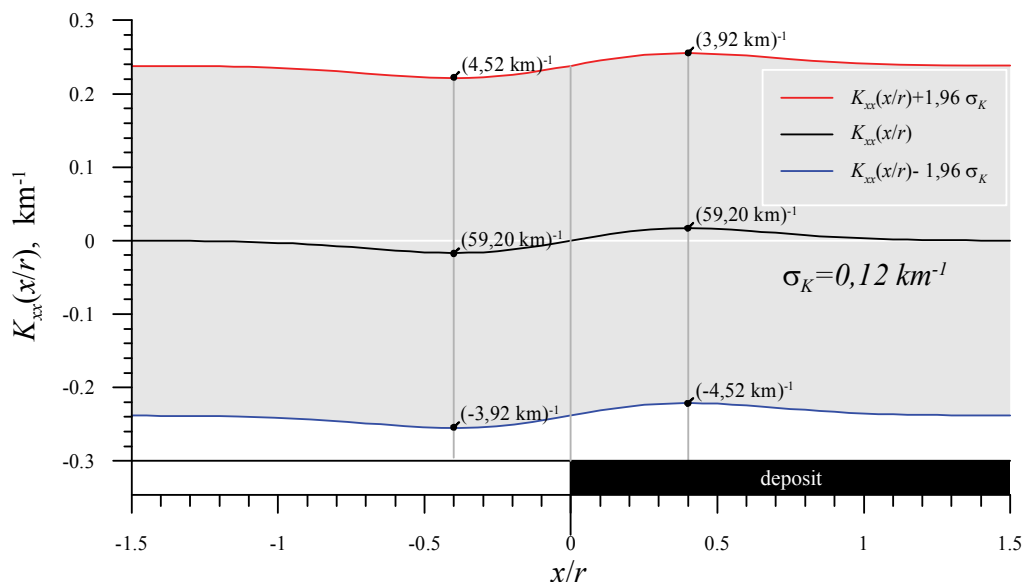


Fig. 6. Chart of curvatures depending on x/r . Marked confidence range includes actual value with probability $1 - \alpha = 0.95$

Left borders of confidence ranges become negative values, what can be explained with an idea that their value reverses in places of extreme values – minimum value appears instead of maximum and inversely.

Figures 2 and 3 show the relation between curvatures (curvatures radius) and parameter of influences dispersion.

When assuming, that standard deviation value σ_w is independent of the building location in relation to mining workings, σ_T, σ_K ill also be independent of such location. Therefore, calculated confidence range applies to the whole exploitation influences area and it can be marked on charts of deformation indicators at T, K (Fig. 4, 5, 6).

6. Conclusion

In order to prepare probabilistic forecast of deformation indicators, especially for curvatures of building's foundations, it is necessary to determine standard, random fluctuation deviations that define the *uncertainty of theory parameters* for these indicators and standard, random fluctuation deviations resulting from *natural dispersion* of such indicators. The knowledge of natural indicators dispersion is limited. This paper points out various possible methods towards the dispersion phenomenon. However, due to the lack of its credible model, it is currently not possible to determine such standard deviations in the case of so-called forecast point deformations.

Therefore, risk assessment of buildings may include section deformation indicators for which the elements of foundation constructions should serve as the length of sections. There are properly determined calculations (5), (6), (7) for standard deviations of their fluctuation result-

ing from their dependence on fluctuation of vertical and horizontal displacements. They can be successfully used for section indicators. As a result, confidence ranges can be determined for such fluctuation for all section deformation indicators.

Even if the forecast point curvatures are small, their values may be greater because of natural dispersion.

References

- Batkiewicz W., 1971. *Odcchylenia standardowe poeksploatacyjnych deformacji górotworu* [Standard deviations of post-mining deformation of rock mass]. Prace Komisji Górnictwo-Geodezyjnej PAN, Geodezja, 10, Kraków.
- Florkowska L., 2011. *Application of numerical nonlinear mechanics in the issues of protecting buildings in mining areas* (in Polish) [Zastosowanie numerycznej mechaniki nieliniowej w zagadnieniach ochrony budynków na terenach górniczych]. Arch. Min. Sci., Monograph, No 11, Kraków.
- Florkowska L., 2012. Building protection against the backdrop of current situation and growth perspectives for polish mining industry [Problematyka ochrony obiektów budowlanych na tle sytuacji I perspektyw rozwoju górnictwa w Polsce]. Arch. Min. Sci., Vol. 57, No 3, p. 645-655.
- Kowalski A., 2007. *Nieuistalone górnicze deformacje powierzchni w aspekcie dokładności prognoz* [Transient mining surface deformations in the prediction accuracy aspect]. The Central Mining Institute Research Papers, No. 871, Katowice.
- Kowalski A., 2014. *Prognozy deformacji powierzchni w świetle deformacji określanych pomiarowo metodami geodezyjnymi* [Forecasting surface deformation in relation to deformation determined by measuring geodetic methods]. Research Paper at ZO SITG Conference in Rybnik, 21.10.2014.
- Kwiatek J. et al., 1997. *Ochrona obiektów budowlanych na terenach górniczych* [Protection of building objects in mining areas]. Monograph, Wyd. GIG, Katowice.
- Kwiatek J., 2006. *Probabilistyczna ocena wpływu krzywizn powierzchni na obiekty budowlane* [Influence of surface curvatures on building in terms of probabilistic assessment]. Przegląd Górnictwy, Vol. 6.
- Kwiatek J., 2007. *Obiekty budowlane na terenach górniczych* [Building objects on mining areas]. Wyd. GIG, Katowice.
- Kwiatek J., 2008. *Ocena bezpieczeństwa obiektów budowlanych poddanych oddziaływaniom górniczym* [Safety assessment of buildings subjected to mining influences]. Research Reports of the Central Mining Institute. Ochrona obiektów budowlanych na terenach górniczych [Safety And Protection Of Building Objects In Mining Areas], Kwartalnik Górnictwa i Środowisko [Quarterly Mining & Environment], Katowice, p. 231-249.
- Ostrowski J., 2006. *Deformacje powierzchni a zagrożenia uszkodzeniami budynków na terenach górniczych w ujęciu probabilistycznym* [Surface deformation and hazard of building damages located in mining areas in the probability aspect]. Rozprawy. Monografie, No. 160, AGH, Kraków.
- Popiołek E., 1976. *Rozproszenie statystyczne odkształceń poziomych terenu w świetle geodezyjnej obserwacji skutków eksploatacji górniczej* [Statistical dispersion of horizontal surface deformations in terms to geodetic observation of mining extraction consequences]. Zeszyty Naukowe AGH, Geodezja, z. 44, Kraków.
- Popiołek E., 1996. *Zależność pomiędzy rozproszeniem losowym procesu deformacji powierzchni terenu a głębokością eksploatacyjną* [Relation between random dispersion of surface deformation process and exploitation depth]. [W:] Materiały VII Międzynarodowego Sympozjum „Geotechnika” - Geotechnics '96. Politechnika Śląska, Wydział Górnictwa i Geologii, Gliwice-Ustroń, 22-25.10.1996, p. 149-155.
- Popiołek E. et al., 1997a. *Losowość pogórniczych deformacji terenu i odporności obiektów powierzchniowych w świetle wyników pomiarów geodezyjnych i obserwacji budowlanych oraz jej wpływów na wiarygodność prognoz szkód górniczych* [Randomness of post-mining deformation and surface building resistance in terms of geodetic measurements and construction observations, and the influence on credibility of mining damages forecast]. Projekt badawczy KBN 9S60102907, Kraków, AGH.
- Popiołek E., Milewski M., Ostrowski J., 1995. *Próba oceny przydatności krzywizny profilu niecki obniżeniowej jako wskaźnika zagrożenia obiektu poddawanego wpływom podziemnej eksploatacji górniczej (na przykładzie LGOM)*

- [Attempt to evaluate value of curvatures of subsidence trough profile as hazard indicator of a building impacted by underground mining exploitation (on the example of LGOM)]. *Przegląd Górnictwy*, Nr 11 (866).
- Popiółek E., Ostrowski J., 1981. *Próba ustalenia głównych przyczyn rozbieżności prognozowanych i obserwowanych poeksploatacyjnych wskaźników deformacji*. [Attempt to determine mining causes of divergence in proposed forecasts and observed post-mining deformation indicators]. Ochrona Terenów Górnictwych, Vol. 58.
- Popiółek E., Ostrowski J., Stoch T., 1997b. *Rozproszenie losowe pogórniczych wskaźników deformacji powierzchni terenu we współczesnych warunkach eksploatacji górniczej w Polsce* [Random dispersion of post-mining deformation indicators in current conditions of mining in Poland]. [W:] Materiały Konferencji Naukowo-Technicznej: „IV Dni Miernictwa Górnictwa i Ochrony Terenów Górniczych”, Rytro, 24-27.09.1997, p. 147-154.
- Popiółek E., Stoch T., 2005. *Rozwój procesu deformacji terenu w aspekcie losowości przebiegu wskaźników deformacji* [Development of land deformation process in terms of random character of development indicators]. [W:] Materiały Konferencji Naukowo-Technicznej: „VIII Dni Miernictwa Górnictwa i Ochrony Terenów Górniczych”, GIG Katowice, Ustroń, 15-17.06.2005, p. 512-524.
- Prusek S., Jędrzejec E., 2008. *Adjustment of the Budryk-Knothe theory to forecasting deformations of gateroads*. Arch. Min. Sci., Vol. 53. No 1, p. 97-114.
- Stoch T., 2005. *Wpływ warunków geologiczno-górniczych eksploatacji złoża na losowość procesu przemieszczeń i deformacji powierzchni terenu* [Influence of mining and geological conditions of mining extraction on randomness of displacement and surface deformation]. Doctoral thesis, AGH, Kraków.

Received: 06 October 2014